Multiple plasmon-induced transparencies in coupled-resonator systems

Jianjun Chen,[1,2,*] Chen Wang,[1,2] Ru Zhang,[1,2] and Jinghua Xiao[1,2]

[1]*State Key Laboratory of Information Photonics and Optical Communications, Beijing University of Posts and Telecommunications, Beijing 100876, China*

[2]*School of Science, Beijing University of Posts and Telecommunications, Beijing 100876, China*

**Corresponding author: chernmore@pku.edu.cn*

Received August 13, 2012; revised October 14, 2012; accepted November 13, 2012; posted November 14, 2012 (Doc. ID 174233); published December 10, 2012

Multiple plasmon-induced transparencies are numerically predicted in an ultracompact plasmonic structure, comprising series of stub resonators side-coupled with a metal-isolator-metal waveguide. Because of the phase-coupled effect, electromagnetically induced transparency (EIT)-like spectral response occurs between two adjacent stub resonators with detuned resonant wavelengths. In this approach, multiple EIT-like spectral responses, with bandwidths of the order of several nanometers, are obtained in the plasmonic structure with a small footprint of about 0.6 μm^2. An analytic model and the relative phase analysis based on the scattering matrix theory are used to explain this phenomenon. © 2012 Optical Society of America

OCIS codes: 240.6680, 230.4555, 060.4230.

Electromagnetically induced transparency (EIT) is a quantum interference effect with a spectrally narrow optical enhanced transmission, which results from a coherent interaction between the ~~atomic levels~~ and the ~~applied optical fields~~ [1]. The enhanced transmission can lead to photons that are slowed down dramatically, which has potential applications in the areas of nonlinearities [2], modulations, and biosensors [3]. Recently, tremendous attention has been attracted to the studies that EIT-like optical responses can be obtained in classical resonator systems [4], which are easily realized and integrated into the chips. As we know, surface plasmon polaritons (SPPs) can be tightly confined by ultrasmall metallic structures beyond the diffractive limits [5] and have many applications [5–7]. Thus, combining the EIT-like optical responses with nanoplasmonic structures would open the possibility of achieving ultracompact functional optical components in highly integrated optics [3,8–14]. For example, engaging plasmonic array (multicell) structures [3,8,9], the EIT-like optical responses were achieved. Recently, using a unit-cell structure with more compact sizes, the EIT-like transmission spectra were also theoretically predicted [10–14] and even experimentally demonstrated [15]. However, all the previous works only presented the results of the single EIT-like optical response in plasmonic structures. This would limit their applications for constructing complex functional optical devices in ultrasmall structures considering that miniaturization and the multifunctionalization of optical devices hold the key to increasing the integrated densities in the next generation of photonic circuits.

In this Letter, multiple EIT-like optical responses are obtained in an ultracompact plasmonic structure, comprising a series of stub resonators side-coupled with a metal-isolator-metal (MIM) waveguide. Herein, the single stub resonator typically exhibits broadband transmission spectra with nearly symmetric Lorentzian-like lineshapes [16,17]. Based on the phase-coupled effect [10], EIT-like spectral responses occur between two adjacent stub resonators with slightly detuned resonant wavelengths. In this approach, multiple EIT-like spectral responses are obtained in the plasmonic structure with a series of stub resonators. An analytic model and the relative phase analysis based on the scattering matrix theory are used to explain this phenomenon. This plasmonic structure with multiple EIT-like spectral responses is of importance for constructing complex functional devices in highly integrated photonic circuits.

The characteristics of the proposed plasmonic structure with multi-stub resonators are investigated with the finite element method (FEM) of Comsol Multiphysics. In the simulations, the metal and dielectric are Ag and air, respectively. The MIM dielectric gap and the stub width and length are assumed to be $t = 50$ nm, $w = 50$ nm, and $d \in 460, 570$ nm, respectively. This single stub resonator can provide a broadband transmission spectrum with bandwidths of about $\Delta\lambda_{\mathrm{FWHM}} \approx 180$ nm. In the proposed structure with multistub resonators, different resonators would couple with each other through the MIM waveguide. It should be pointed out that these structure sizes are much smaller than the SPP propagation length, so the propagation loss can be neglected [13,16].

To investigate this coupling effect between the stub resonators, the transmission characteristics of two stub resonators with different resonator lengths ($d = 500$ nm and $d = 535$ nm) [inset in Fig. 1(a)] were calculated first, and the results are shown in Fig. 1(a). The calculated method can be seen in our previous work [17]. It was found that a narrow transmission peak emerges in the broadband transmission spectrum when the separation of the stub resonators is $L = 370$ nm. This is a typical EIT-like optical response [10–15]. The SPPs are completely reflected when the stub resonator is exactly at resonance, as shown in Figs. 1(b) and 1(d). Near the resonant wavelengths, the SPPs can be highly reflected by the stub resonators, acting as a high reflector [13,16,17]. Thus, the SPPs can be reflected back and forth off the two stub resonators with high reflectivity, constructing a Fabry–Perot (FP) resonator [10] in the plasmonic system. This results in the narrow transmission peak at $\lambda = 1001$ nm in the transmission spectra. The corresponding field distribution at $\lambda = 1001$ nm is shown in Fig. 1(c). Stronger

field distributions than those in Figs. 1(b) and 1(d) are obviously observed. This serves as direct evidence that the resonant enhancement occurs in the FP resonator.

Adding another resonator ($d = 570$ nm) in the right side of the two-resonator-coupled structure, a three-resonator-coupled system is constructed, as shown by the inset in Fig. 2(a). By carefully adjusting the separation of the right two resonators to be $L = 390$ nm, two equal transmission peaks (at about $\lambda = 999$ nm and $\lambda = 1062$ nm) obviously emerge, revealing two EIT-like optical responses, as shown in Fig. 2(a). For the same reason as the two-resonator-coupled case, here each two adjacent stub resonators can construct an FP resonator in the three-resonator-coupled systems [10]. The corresponding field distributions at these two transmission peaks are displayed in Figs. 2(b) and 2(c). At $\lambda = 999$ nm (or $\lambda = 1062$ nm), the left (or right) two stub resonators together with the MIM part between them have strong field distributions, as shown in Fig. 2(b) or 2(c). This means the resonant enhancement occurs in the FP resonators, resulting in the transmission peaks.

The above principle can be generalized to the multi-resonator-coupled system. For example, in the four-resonator-coupled system, placing a fourth stub resonator ($d = 465$ nm) at the left side with the separation of 335 nm to the three-resonator-coupled system [inset in Fig. 3(a)], three transmission peaks occur in the broadband transmission spectrum, revealing a three-EIT-like optical response [Fig. 3(a)]. These narrow resonant spectra in the three-EIT-like optical response exhibit a bandwidth of only about $\Delta\lambda'_{\mathrm{FWHM}} = 6$ nm, which is much smaller than that ($\Delta\lambda_{\mathrm{FWHM}} \approx 180$ nm) in the single stub resonator. The corresponding field distributions at these transmission peaks are displayed in Figs. 3(b)–3(d). These strong field distributions also reveal that the transmission peaks result from the resonant enhancements in the FP resonators [10]. More EIT-like peaks can be obtained by adding more stub resonators (≥5 resonators) in the plasmonic structure. The multiresonator-coupled system with multi-EIT-like optical responses and ultracompact sizes may have complex functional applications, such as channel selection, channel add–drop, multichannel bandpass filtering, multichannel switches, wavelength-division multiplexing, and interleavers.

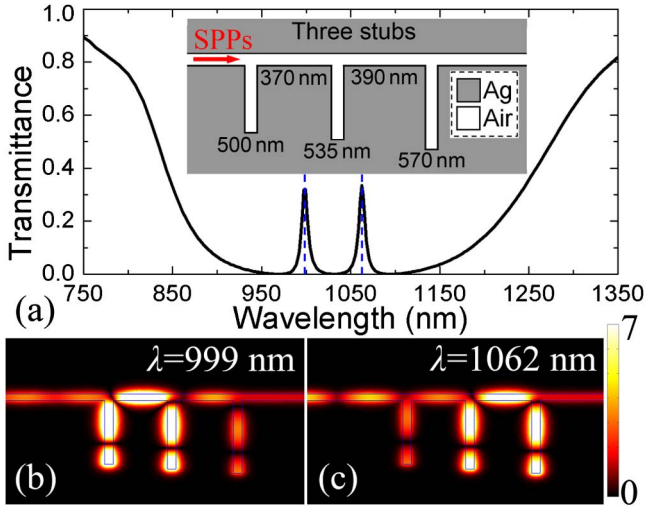

Fig. 2. (Color online) (a) Transmission spectrum of the three-resonator-coupled system. Inset shows the schematic of the three-resonator-coupled system and the geometrical parameters. Field distributions (|Hz|) of SPPs in the system at (b) $\lambda = 999$ nm, and (c) $\lambda = 1062$ nm.

To test the analysis above, an analytic model based on the scattering matrix theory [17,18] is used to explain the transmission spectra in the proposed system. Quantitatively, the scattering property of the single stub resonator for the incident SPPs at a frequency of $\omega = c/\lambda$ can be given by a transfer matrix of T_S [17,18]:

$$\begin{bmatrix} A_{Ob} \\ A_{Ib} \end{bmatrix} = T_S^m \begin{bmatrix} A_{Ia} \\ A_{Oa} \end{bmatrix} = \begin{bmatrix} 1 - \frac{i\delta}{\omega-\omega_0} & \frac{-i\delta}{\omega-\omega_0} \\ \frac{i\delta}{\omega-\omega_0} & 1 + \frac{i\delta}{\omega-\omega_0} \end{bmatrix} \begin{bmatrix} A_{Ia} \\ A_{Oa} \end{bmatrix}, \tag{1}$$

where the superscript ($m = 1, 2, 3\ldots$) in T_S^m denotes the mth stub resonator in the plasmonic system; c is the

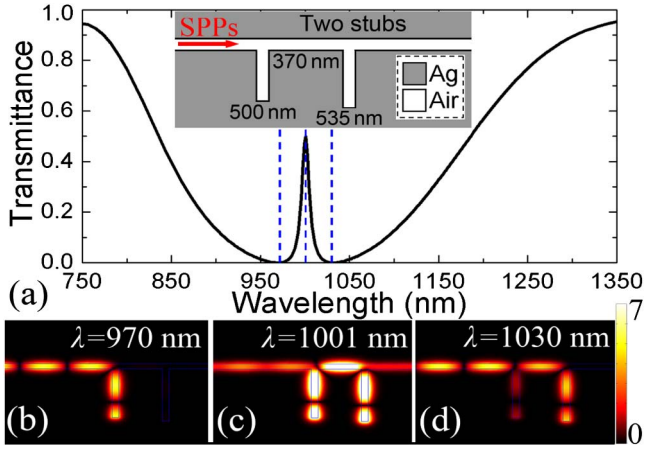

Fig. 1. (Color online) (a) Transmission spectrum of the two-resonator-coupled system. Inset shows the schematic of the two-resonator-coupled system and the geometrical parameters. Field distributions (|Hz|) of the SPPs in the two-resonator-coupled system at (b) $\lambda = 970$ nm, (c) $\lambda = 1001$ nm, and (d) $\lambda = 1030$ nm.

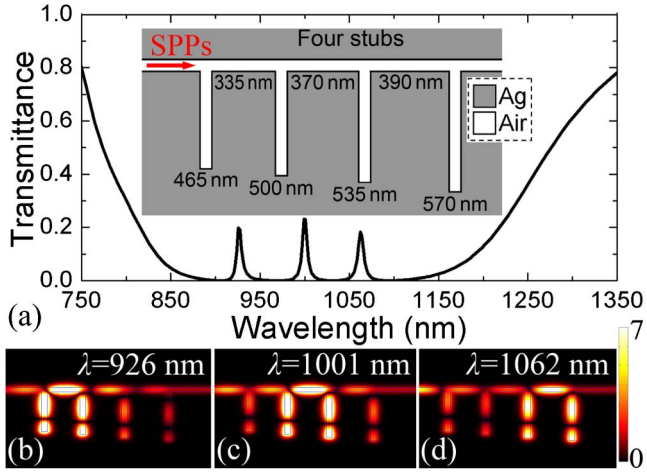

Fig. 3. (Color online) (a) Transmission spectrum of the four-resonator-coupled system. Inset shows the schematic of the four-resonator-coupled system and the geometrical parameters. Field distributions (|Hz|) of SPPs in the system at (b) $\lambda = 926$ nm, (c) $\lambda = 1001$ nm, and (d) $\lambda = 1062$ nm.

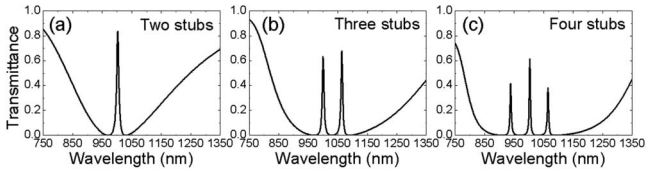

Fig. 4. Analytic model results of the transmission spectra for (a) two stubs, (b) three stubs, and (c) four stubs systems.

velocity of light in vacuum; $\omega_0 = c/\lambda_0$ and $2\delta = c\Delta\lambda_{\mathrm{FWHM}}/\lambda_0^2$ are the resonant frequency and the width of the resonance in the stub resonator coupled with the MIM waveguide, respectively; A_{Ij}, and A_{Oj} $(j = a, b)$ are the incoming and outgoing SPP amplitudes on one side of the stub resonator.

For the phase shift coming from the SPPs propagating from the mth stub to the nth stub along the MIM waveguide, the transfer matrix $\boldsymbol{T_p}$ has the form of [17,18]

$$T_p^{mn} = \begin{bmatrix} \exp(i\varphi) & 0 \\ 0 & \exp(-i\varphi) \end{bmatrix}, \tag{2}$$

where, $\varphi = 2\pi n_{\mathrm{eff}} L_{mn}/\lambda$ is the accumulated phase shift for SPPs propagating from the mth stub to the nth stub; L_{mn} is the separation between the two stubs; and n_{eff} is the effective refractive index of SPPs in the MIM waveguide. Therefore, the transfer matrix of T_{all} for the multiresonator-coupled system can be expressed as

$$T_{\mathrm{all}} = T_s^1 \times T_p^{12} \times T_s^2 \times T_p^{23} \times T_s^3 \times \cdots. \tag{3}$$

In the system, the transmittance is determined by $|1/T_{\mathrm{all},22}|^2$. The calculated transmission spectra of the two-, three-, and four-resonator-coupled systems using the analytic model are displayed in Figs. 4(a)–4(c), respectively. It is observed that these results agree well with the FEM simulation results. In the calculations, $n_{\mathrm{eff}} \approx 1.38 + 0.002i$ were obtained from the FEM simulations at $\lambda = 1000$ nm; the resonant wavelengths in each single stub resonator (with the bandwidth of $\Delta\lambda_{\mathrm{FWHM}} = 180$ nm) are 910, 970, 1030, and 1090 nm, respectively; and the separations of every two adjacent stubs are 340, 365, and 385 nm, respectively.

Moreover, from Eq. (1), we can get that the m-stub cavity resonator can reflect SPPs with an amplitude reflectivity of $r_s = |T_{s,21}/T_{s,22}|$ and a phase shift of $\theta_m = \arctan[\mathrm{Im}(T_{s,21}/T_{s,22})/\mathrm{Re}(T_{s,21}/T_{s,22})]$. Thus, the SPPs can be reflected back and forth off the two adjacent stubs, constructing an FP resonator [10]. The accumulated phase delay per round trip in the FP resonator is

$$\varphi_{mn}(\lambda) = 4\pi n_{\mathrm{eff}} L_{mn}/\lambda + \theta_m + \theta_n. \tag{4}$$

For every two adjacent stub resonators in the system, we can obtain $\varphi_{12}(\lambda = 940\ \mathrm{nm}) = \varphi_{23}(\lambda = 1000\ \mathrm{nm}) = \varphi_{34}(\lambda = 1060\ \mathrm{nm}) = 2\pi$. This reveals a constructive interference in the FP resonator, giving rise to the transmission peaks at these wavelengths. It should be pointed out that the relative phase analysis agrees well with both the simulation model and analytical model. Although the small variations of the structure parameters can greatly influence the EIT-like spectra [10,13,15], the analytic model and the phase analysis can help to find the proper parameters to obtain the desired EIT-like spectra.

In summary, multiple EIT-like optical responses in an ultracompact plasmonic structure with a series of stub resonators were numerically predicted. An analytic model and the relative phase analysis based on the scattering matrix theory were used to explain this phenomenon, which matched well with the FEM simulation results. This ultracompact structure, which can give rise to multiple EIT-like spectral responses with bandwidths of the order of several nanometers, has many important applications in complex functional optical devices. Moreover, the analytical model and the relative phase analysis can provide guidance for designing compact and complex functional plasmonic devices.

This work was supported by the National Natural Science Foundation of China (Grant Nos. 11204018, 61177085, and 51172030) and the National Basic Research Program of China (Grant No. 2010CB923200).

References

1. K. J. Boller, A. Imamoglu, and S. E. Harris, Phys. Rev. Lett. **66**, 2593 (1991).
2. S. E. Harris, J. E. Field, and A. Imamoglu, Phys. Rev. Lett. **64**, 1107 (1990).
3. N. Liu, L. Langguth, T. Weiss, J. Kastel, M. Fleischhauer, T. Pfau, and H. Giessen, Nat. Mater. **8**, 758 (2009).
4. K. Totsuka, N. Kobayashi, and M. Tomita, Phys. Rev. Lett. **98**, 213904 (2007).
5. D. K. Gramotnev and S. I. Bozhevolnyi, Nat. Photon. **4**, 83 (2010).
6. Z. Zang, K. Mukai, P. Navaretti, M. Duelk, C. Velez, and K. Hamamoto, Appl. Phys. Lett. **100**, 031108 (2012).
7. J. J. Chen, Z. Li, S. Yue, and Q. H. Gong, Nano Lett. **11**, 2933 (2011).
8. S. Zhang, D. A. Genov, Y. Wang, M. Liu, and X. Zhang, Phys. Rev. Lett. **101**, 047401 (2008).
9. J. Zhang, W. L. Bai, L. K. Cai, Y. Xu, G. F. Song, and Q. Q. Gan, Appl. Phys. Lett. **99**, 181120 (2011).
10. R. D. Kekatpure, E. S. Barnard, W. Cai, and M. Brongersma, Phys. Rev. Lett. **104**, 243902 (2010).
11. Y. R. He, H. Zhou, Y. Jin, and S. L. He, Appl. Phys. Lett. **99**, 043113 (2011).
12. Y. Zhang, S. Darmawan, L. Y. M. Tobing, T. Mei, and D. H. Zhang, J. Opt. Soc. Am. B **28**, 28 (2011).
13. Z. Han and S. I. Bozhevolnyi, Opt. Express **19**, 3251 (2011).
14. H. Lu, X. M. Liu, D. Mao, Y. K. Gong, and G. X. Wang, Opt. Lett. **36**, 3233 (2011).
15. J. J. Chen, Z. Li, S. Yue, J. H. Xiao, and Q. H. Gong, Nano Lett. **12**, 2494 (2012).
16. J. J. Chen, Z. Li, J. Li, and Q. H. Gong, Opt. Express **19**, 9976 (2011).
17. J. J. Chen, Z. Li, M. Lei, X. L. Fu, J. H. Xiao, and Q. H. Gong, Plasmonics **7**, 441 (2012).
18. H. A. Haus, *Waves and Fields in Optoelectronics* (Prentice–Hall, 1984).